Japan Bilingual Publishing Co.

Transportation Development Research
https://ojs.bilpub.com/index.php/tdr

COMMUNICATION

Low-Drag Bodies of Revolution and Their Applications for Effective Transportation

Igor Nesteruk [1,2*]

[1] *Institute of Hydromechanics, National Academy of Sciences of Ukraine, Kyiv 03680, Ukraine*
[2] *Isaac Newton Institute for Mathematical Sciences, University of Cambridge, Cambridge CB3 0EH, UK*

ABSTRACT

Improving the shape of vehicle hulls remains a pressing task, particularly in minimizing harmful emissions into the environment and achieving optimal economic performance. To reduce aerodynamic or hydrodynamic drag, special body shapes can be recommended that provide a flow pattern without boundary-layer separation. Corresponding bodies of revolution were calculated with the use of slender body theory and exact solutions of Euler equations. Some of them were successfully tested in the wind tunnels. It was demonstrated that the flow pattern can be laminar at relatively high Reynolds numbers, and the volumetric drag coefficient on such bodies does not depend on the shape, but rather decreases with an increase in the volumetric Reynolds number. The critical values of the Reynolds number were estimated, and the simple relationship for critical values of velocity, volume, and length was obtained, which allows estimating the parameters of a minimal drag hull and the maximum speed of aquatic animals. In particular, the Gray paradox was resolved, and the very high speed of the sailfish was explained. It was also shown that hulls with sharp concave noses have no stagnation points, pressure, and temperature peaks. In supersonic flows, they can reduce overheating of the noses. Such hulls penetrating water have much lower loads on the noses. Moving on the water surface, such hulls can ensure a low wave resistance and total drag. The proposed hull shapes could significantly reduce

*CORRESPONDING AUTHOR:
Igor Nesteruk, Institute of Hydromechanics, National Academy of Sciences of Ukraine, Kyiv 03680, Ukraine; Isaac Newton Institute for Mathematical Sciences, University of Cambridge, Cambridge CB3 0EH, UK; Email: inesteruk@yahoo.com

ARTICLE INFO
Received: 18 August 2025 | Revised: 28 September 2025 | Accepted: 9 October 2025 | Published Online:17 October 2025
DOI: https://doi.org/10.55121/tdr.v3i2.697

CITATION
Nesteruk, I., 2025. Low-Drag Bodies of Revolution and Their Applications for Effective Transportation.Transportation Development Research. 3(2): 1–8. DOI: https://doi.org/10.55121/tdr.v3i2.697

the drag of underwater vehicles, SWATH and floating ships, airplanes, airships, cars, and gliders. The use of critical values of parameters allows developing the vehicles with the high commercial efficiency (weight-to-drag ratio) and range.

Keywords: Drag Reduction; Unseparated Shapes; Laminar-Turbulent Transition; Grey Paradox; Hull Overheating; Water Penetration

1. Introduction

To minimize carbon emissions and achieve the high economic performance, the shape of a vehicle has to be improved [1–8]. To reduce the drag, special body shapes can be recommended that provide a flow pattern without boundary-layer separation [7,9]. Corresponding bodies of revolution were calculated with the use of the slender body theory and exact solutions of Euler equations [9–12] and tested in the wind tunnels [9,13]. In this short communication, we will briefly analyze the results presented by Nesteruk and co-authors [4,6,9–17] and discuss the perspectives of using the presented shapes for effective transportation.

2. Materials and Metods

For elongated bodies of revolution ($D/L<<1$; L is its length; D is the maximum diameter) moving at constant speed U along the axis of symmetry x, the flow plow pattern can be simulated with the use of slender body theory [9]. In the unbounded incompressible flow, the radius $R(x)$ of the body and the pressure coefficient $C_p\ (x)$ on its surface are related by the first approximation equation [9]:

$$\frac{d^2R^2}{dx^2} = -\frac{Cp(x)}{ln\varepsilon}. \quad (1)$$

For bodies moving near the water surface, the pressure distributions and velocities on the water surface were calculated using the distributions of sources and sinks [12,15,16]. For compressible flow, the temperature on the body surface was calculated [11,15]. To improve the accuracy, the exact solutions of the Euler equations have been used [9–12,15]. To support the theoretical results, the wind tunnel tests were performed [9,13].

3. Results and Discussion

3.1. No Separation on Special-Shaped Bodies

Eq. (1) enables calculating the shape of the bodies with a prescribed pressure distribution on their surface. To avoid separation of the boundary, the special-shaped bodies of revolution with negative pressure gradients were calculated with the use of the exact solution of the Euler equations as well (see examples in **Figures 1** and **2**). Wind tunnel tests have confirmed the absence of separation on some bodies of revolution [9,13] (see **Figure 2**) similar to the trunks of aquatic animals, which also ensure a flow pattern without separation [18,19].

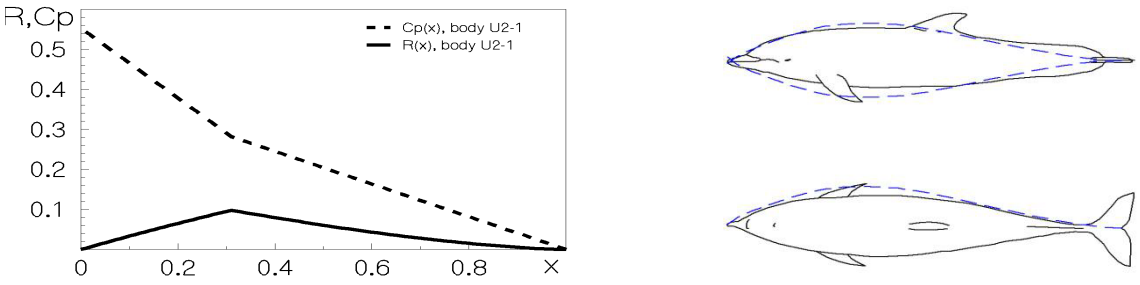

(**a**) (**b**)

Figure 1. (**a**) Axisymmetric bodies with negative pressure gradients on their surfaces. First approximation equation and its solution [9]; (**b**) Exact solution of Euler equations and comparison with the dolphin body shape [9,10].

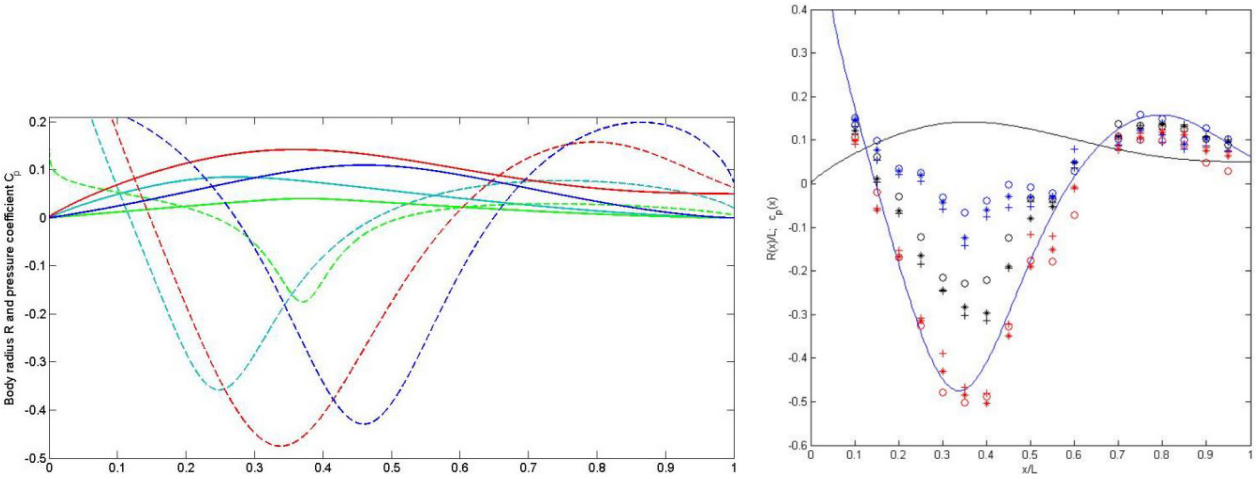

(**a**) (**b**)

Figure 2. (**a**) Radii of axisymmetric bodies (solid lines) and pressure coefficients *Cp* (dashed curves) versus dimensionless axis coordinate *x/L*. Body UA-12.4c "Sailfish" (*L/D*=12.4; green lines); UA-5.9c "Blue shark" (*L/D*=5.9; blue lines); UA-4.5c "Albacore" (*L/D*=4.5; dark blue lines) and the unclosed body UA-2 (*L/D*=3.52; red lines) [10]. (**b**) Measurements of the pressure coefficient on the body UA-2 (markers), theory (the blue line) available in the study of Nesteruk et al. [13].

3.2. No Turbulence on Slender Unseparated Shapes at Low Reynolds Numbers

When the Reynolds numbers are small enough, the boundary-layer on a flat plate remains laminar for any frequencies of disturbances (according to the Tollmin-Schlichting-Lin theory [20]). Mangler-Stepanov transformations [20] allowed us to estimate the critical value of the Reynolds number for a slender unseparated body of revolution as follows [4]:

$$Re_L^* = \frac{59558\pi L^3}{V} \tag{2}$$

With the use of critical values of the velocity U^*, volume V^*, and length L^*, relationship (2) can be rewritten as follows:

$$U^*V^* = 1.87 \times 10^5 \nu (L^*)^2 \tag{3}$$

(ν is the kinematic viscosity of air or water). Eq. (3) yields the parameters of a minimal drag hull (since the volumetric drag coefficient is minimal at the critical Reynolds number [4]) and allows estimating the maximum speed of aquatic animals. E.g., the dolphin's body of volume 0.0907 m^3 and the length 1.83 m (these values were used by Grey [21] to estimate the drag) yields the critical value of the velocity 8.9 m/s in water with the temperature15 °C. This fact resolves the Grey paradox [21,22], since this animal can ensure laminar boundary layer on its entire surface at U < 8.9 m/s. For slenderer bodies (with higher values of the length-to-diameter ratio), the critical Reynolds numbers are larger and the corresponding volumetric drag coefficients are much lower in comparison with the standard shapes [23] or special low-drag bodies of revolution proposed before by different authors [24–26]. For example, the sailfish (Istiophorus platypterus; which probably is the fastest fish with the maximal speed 33 m/s [18]) can ensure the laminar flow pattern at speeds less than 42 m/s for the length 3.15 m and mass 56 kg (according to (3)).

3.3. Minimal Friction Drag on Slender Axisymmetric Unseparated Hulls

On a slender body of revolution with the laminar attached boundary layer, the volumetric drag coefficient is independent of the body shape and related to the volumetric Reynolds number as follows [4,10]:

$$C_V = \frac{4.7}{\sqrt{Re_V}}, \quad Re_V = \frac{UV^{\frac{1}{3}}}{\nu} \tag{4}$$

In **Figure 3**, the black line represents the first relationship (4) and demonstrates that the drag coefficient in the unbounded flow of incompressible fluid can be very small at high values of the critical Reynolds number (2), exceeding which leads to turbulence and deviation from

dependence (4). Since critical Reynolds numbers are higher for slenderer bodies of revolution (according to eq. (2)), elongated hulls ($L/D>>1$) could significantly reduce the drag of underwater vehicles, SWATH ships, airplanes, airships, cars, air and sea gliders, bikes, etc., as mentioned in Nesteruk [4,6] and Nesteruk et al. [14,17].

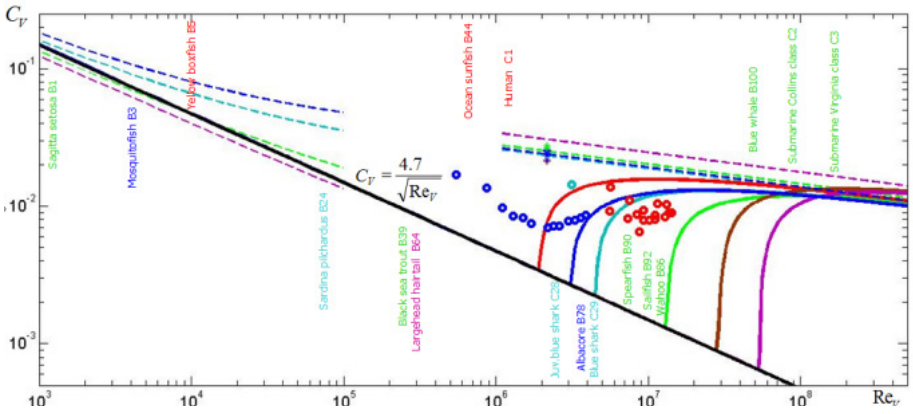

Figure 3. Drag coefficients versus volumetric Reynolds numbers (both based on the volume of the body of revolution). Dashed curves and "stars" correspond to theoretical and experimental values of drag on standard shapes, solid lines represent eq. (4) and turbulent drag on the special-shaped axisymmetric hulls [4,10]. Dark blue lines represent bodies with L/D = 4.5; blue curves - L/D = 5.9; green - L/D = 12.4; magenta - L/D = 33.3. The solid brown line corresponds to the special-shaped unclosed body UA-23.3 (L/D = 23.3) [10]. "Circles" show the experimental data for special-shaped bodies of revolution proposed by other authors [24–26]. Names of aquatic animals represent values of volumetric Reynolds numbers typical for their locomotion.

Use of the laminar hulls increases the commercial efficiency (weight-to-drag ratio k) and the range with a fixed energy reserve on board [4,6]. In particular, for the maximal range of electrical vehicles S_e can be estimated as follows [6]:

$$S_e \sim 10\ km \tag{5}$$

Since the weight of vehicles is proportional to their volume, the use of critical values of parameters (according to eq. (3)) allows achieving the maximal commercial efficiency.

Eq. (3) could be useful for engineers developing small unmanned vehicles, since the hull volume is rather limited, especially for underwater devices, due to much smaller kinematic viscosity in comparison with air. Nevertheless, a special-shaped hull of a small electrical submarine with a weight 1.6 t and a length 10m can ensure a laminar flow pattern at speeds up to 15 m/s, k = 80.2, and a range up to 800 km [6]. For an airship with L = 50 м and U=20 м/с moving at an attitude 20 km, eq. (3) yields the value of critical hull volume V^* = 3620 м^3, weight 322 kg, and ratio D/L = 0.3. An unseparated shape similar to the body of revolution UA-2c [9] can be used to achieve the economical efficiency k = 226. As estimated by Nesteruk [6], the flight of such an airship can be maintained for an practically unlimited time with the use of solar batteries.

It is impossible to satisfy condition (3) for large or fast vehicles. Then the high turbulent drag (see **Figure 3**) decreases the commercial efficiency. For very small and/or slow vehicles (e.g., sea gliders [6]), the left part of eq. (3) is much smaller than the right one. Nevertheless, small values of speed ensure very high commercial efficiencies and ranges with the use special- shaped hulls proposed by Nesteruk [4,9,10] and shown in **Figure 2a**. The use of well-shaped underwater wings allows obtaining fully laminar sea gliders [4].

Condition (3) is not of fundamental importance for airplanes, since the main contribution to their drag is made not by the fuselage, but by the wings [4,6]. The principles of the optimal wing design are discussed by Nesteruk [4,6]. At the same time, in the conditions of competition, aircraft fuselages should be selected in accordance with formula (3), where possible, and the special unseparated shapes have to be used (see examples in the study of Nesteruk [9–11]).

3.4. No Stagnation Points on Concave Noses. Reduction of Wave Resistance, Loads and Overheating

The shapes of the fastest fish have sharp concave nos-

es [18]. The exact solution for the unbounded flow of inviscid incompressible fluid demonstrated that there are no stagnation points and pressure peaks at the leading edge of similar shapes [11] (see **Figures 4** and **5**). Some approximate approaches have also been used to take into account the presence of the water surface and the fluid compressibility [12,15].

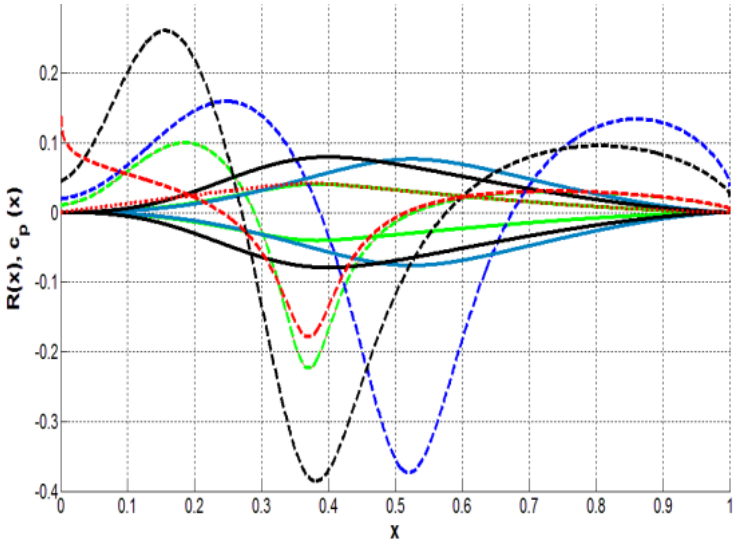

Figure 4. Bodies of revolution with the sharp concave noses (solid green, blue, and black lines) and an example with a convex nose (the red dotted curve). Corresponding pressure distributions are shown by dashed lines [11].

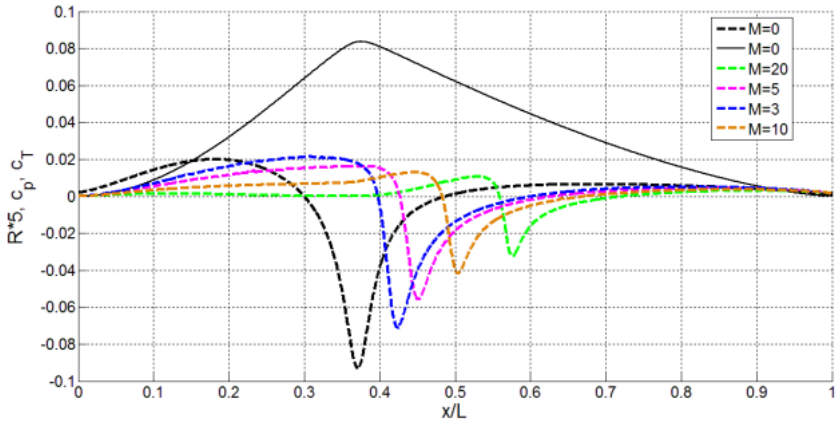

Figure 5. Radius of the slender body of revolution with the concave nose (the black solid curve) and the pressure/temperature coefficients distributions at different values of Mach number (dashed lines) [11].

Sharp concave noses allow avoiding their overheating in hypersonic flows (see Figure 5 [11]). Such hulls penetrating water have much lower loads on the noses (see Figure 4 [11]) and no stagnation points on hulls moving near the water surface along the axis of symmetry (see Figure 6 [12,15]). Since pressure peaks corresponding to stagnation points cause the wave resistance [27], it can be reduced without using any bulbous bows [16]. The possibility of reducing the wave resistance is also evidenced by vertical velocities calculated on the water surface and shown in Figure 7. These velocities and corresponding deformations of the water surface are much lower for hulls with concave noses in comparison with convex ones. After corresponding testing, the proposed new shapes with sharp concave noses can be used as parts of hulls for floating vehicles (boats, ships, etc.). For example, the new special-shaped pontoons can significantly improve the characteristics of the water bikes [17]. For a boat with a displacement 2 m^3 and a speed 15 m/s, the use of a special hull with a concave nose and L = 15.9 m, L/D = 16.8, yields a very high level of the commercial efficiency k = 126 [6]. According to formula (4), the range of the electrical boat with such a hull can exceed 1200 km.

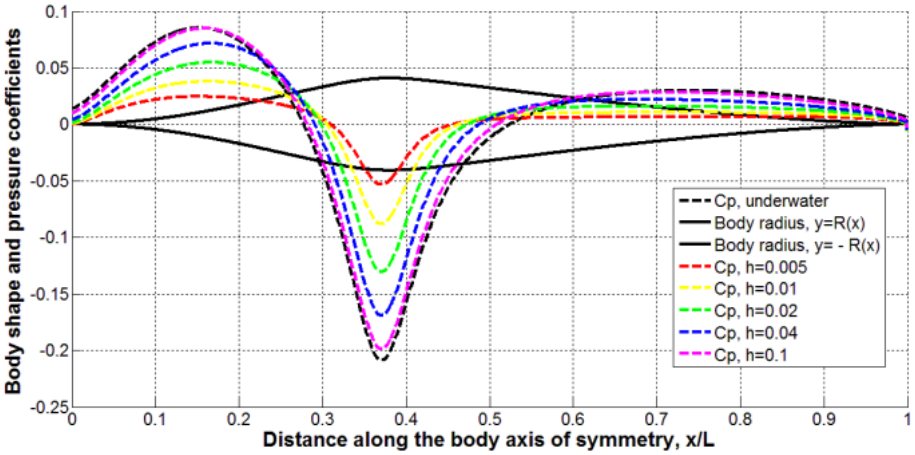

Figure 6. Slender axisymmetric body of revolution with the concave nose. Shape (solid) and pressure coefficients (dashed lines) at different values of dimensionless depth of motion h (based on L) [12].

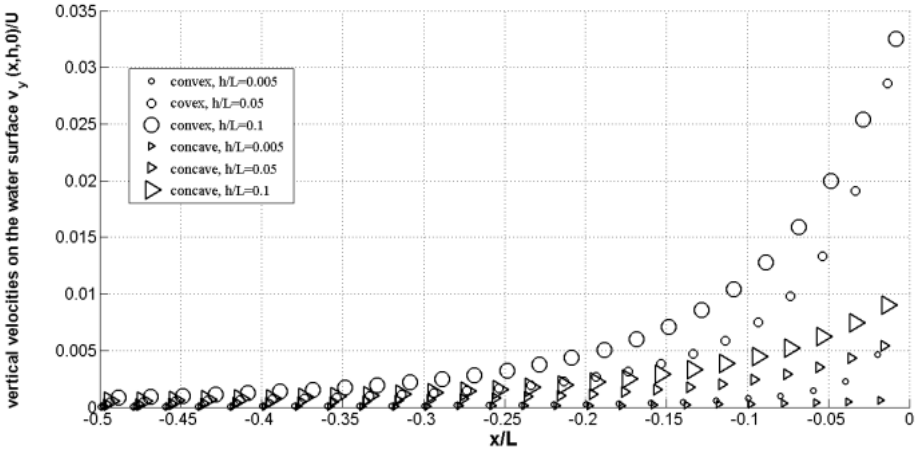

Figure 7. Comparison of two hulls with concave ("triangles") and convex ("circles") noses and L/D = 5.3. Vertical upstream velocities on the water surface at different depths of movement h/L [15].

4. Conclusions

Special shaped bodies of revolution without boundary-layer separation can delay the laminar-turbulent transition, reduce the drag, loading, and overheating, and can be recommended for hulls of underwater and floating vehicles, SWATH ships, airplanes, airships, cars, air and sea gliders. The use of proposed critical values of parameters allows developing the vehicles with the maximum commercial efficiency (weight-to-drag ratio) and the range. Improved vehicles can make a significant contribution to optimizing transportation systems. As a topic for further research, we can propose further improving the separation, noise, and cavitation characteristics of 2D profiles using the shapes with negative pressure gradients proposed by Nesteruk [9].

Funding

This work received no external funding.

Institutional Review Board Statement

Not applicable.

Informed Consent Statement

Not applicable.

Data Availability Statement

Some reported results can be found in papers listed in the text and in the preprint. Available from: https://www.sciencedirect.com/science/article/pii/S0029801820306521?via%3Dihub.

Acknowledgments

The author is grateful to Ulrike Tillmann, James Robinson, Robin Thompson, Matt Keeling, Peter Thomas, Thorsten Möller, Paul Brown, Mykola Losev, Oleksii Rodionov, and INI-LMS Solidarity Programme at the University of Warwick, UK.

Conflicts of Interest

The author declares no conflict of interest.

References

[1] Rehman, F.U., Huang, L., Anderlini, E., et al., 2021. Hydrodynamic modelling for a transportation system of two unmanned underwater vehicles: semi-empirical, numerical and experimental analyses. Journal of Marine Science and Engineering. 9(5), 500. DOI: https://doi.org/10.3390/jmse9050500

[2] Liu, S., Du, C., Han, Y., et al., 2024. Research on hydrodynamics of trans-media vehicles considering underwater time-varying attitudes. Journal of Marine Science and Engineering. 12(8), 1338. DOI: https://doi.org/10.3390/jmse12081338

[3] Suresh Behara, S., Arnold, A., Martin, J.E., et al., 2020. Experimental and computational study of operation of an amphibious craft in calm water. Ocean Engineering. 209, 107460. DOI: https://doi.org/10.1016/j.oceaneng.2020.107460

[4] Nesteruk, I., 2016. Efficiency of steady motion and its improvement with the use of unseparated and supercavitating flow patterns. KPI Science News. 6, 51–67. DOI: https://doi.org/10.20535/1810-0546.2016.6.81605

[5] Liu, B., Xu, X., Pan, D., et al., 2023. Research on shipping energy-saving technology: hydrofoil amphibious vehicle driven by waterjet propulsion. Journal of Cleaner Production. 382, 135257. DOI: https://doi.org/10.1016/j.jclepro.2022.135257

[6] Nesteruk, I., 2024. Shape optimization principles for long-range unmanned vehicles. KPI Science News. 137(1–4), 49–61. DOI: https://doi.org/10.20535/kpisn.2024.1-4.314223 (in Ukrainian)

[7] Abbas, A., de Vicente, J., Valero, E., 2013. Aerodynamic technologies to improve aircraft performance. Aerospace Science and Technology. 28(1), 100–132. DOI: https://doi.org/10.1016/j.ast.2012.10.008

[8] Berger, T., Farhat, M., 2025. Gyroid as a novel approach to suppress vortex shedding and mitigate induced vibration. Scientific Reports. 15, 25777. DOI: https://doi.org/10.1038/s41598-025-11199-0

[9] Nesteruk, I., 2014. Rigid bodies without boundary-layer separation. International Journal of Fluid Mechanics Research. 41(3), 260–281. DOI: https://doi.org/10.1615/InterJFluidMechRes.v41.i3.50

[10] Nesteruk, I., 2019. Maximal speed of underwater locomotion. Innovative Biosystems and Bioengineering. 3(3), 152–167. DOI: https://doi.org/10.20535/ibb.2019.3.3.177976

[11] Nesteruk, I., 2020. Fastest fish shapes and optimal supercavitating and supersonic bodies of revolution. Innovative Biosystems and Bioengineering. 4(4), 169–178. DOI: https://doi.org/10.20535/ibb.2020.4.4.215578

[12] Nesteruk, I., 2022. Shapes of the fastest fish and optimal underwater and floating hulls. Theoretical and Applied Mechanics Letters. 12(1), 100378. DOI: https://doi.org/10.1016/j.taml.2022.100378

[13] Nesteruk, I., Bruehl, M., Moeller, T., 2018. Testing a special shaped body of revolution similar to dolphins' trunk. KPI Science News. 2, 44–53. DOI: https://doi.org/10.20535/1810-0546.2018.2.129140

[14] Nesteruk, I., Krile, S., Koboevic, Z., 2020. Electrical swath ships with underwater hulls preventing the boundary layer separation. Journal of Marine Science and Engineering. 8(9), 652. DOI: https://doi.org/10.3390/jmse8090652

[15] Nesteruk, I., 2024. Special shaped low drag bodies of revolution without boundary-layer separation and stagnation points on the noses. In Proceedings of the Topical Problems of Fluid Mechanics 2024, Prague, Czech Republic, 21–23 February 2024; pp. 21–23. DOI: https://doi.org/10.14311/TPFM.2024.021

[16] Nesteruk, I., 2024. Special-shaped low-drag laminar hulls to increase speed and improve the commercial efficiency of floating vehicles. Hydrodynamics and Acoustics. 3(93)(3), 311–329. DOI: https://doi.org/10.15407/jha2024.03.311

[17] Nesteruk, I., Krile, S., Moeller, T., 2023. Improved low-drag pontoons for water bikes. Journal of Marine Science and Engineering. 11(9), 1754. DOI: https://

doi.org/10.3390/jmse11091754

[18] Aleyev, Y.G., 1977. Nekton. Dr. W. Junk Publishers: The Hague, Netherlands.

[19] Rohr, J., Latz, I., Fallon, S., et al., 1998. Experimental approaches towards interpreting dolphin stimulated bioluminescence. Journal of Experimental Biology. 201(9), 1447–1460.

[20] Loitsyanskiy, L.G., 1995. Mechanics of Liquids and Gases, 6th ed. Begell House: New York, NY, USA.

[21] Gray, J., 1936. Studies in animal locomotion VI. The propulsive powers of the dolphin. Journal of Experimental Biology. 13(2), 192–199.

[22] Bale, R., Hao, M., Bhalla, A., et al., 2014. Gray's paradox: A fluid mechanical perspective. Scientific Reports. 4, 5904. DOI: https://doi.org/10.1038/srep05904

[23] Hoerner, S.F., 1965. Fluid-Dynamic Drag. Hoerner Fluid Dynamics: Midland Park, NJ, USA.

[24] Greiner, L., 1967. Underwater Missile Propulsion. Compass Publications: Washington, DC, USA.

[25] Goldschmied, F.R., 1982. Integrated hull design, boundary layer control and propulsion of submerged bodies: wind tunnel verification. In Proceedings of the AIAA/SAE/ASME 18th Joint Propulsion Conference, Cleveland, OH, USA, 21–23 June 1982; pp. 3–18.

[26] Hansen, R.J., Hoyt, J.G., 1984. Laminar-to-turbulent transition on a body of revolution with an extended favorable pressure gradient forebody. Journal of Fluids Engineering. 106(2), 202–210.

[27] Zeng Q., Hekkenberg, R., Thill, C., et al., 2020. Scale effects on the wave-making resistance of ships sailing in shallow water. Ocean Engineering. 212, 107654. DOI: https://doi.org/10.1016/j.oceaneng.2020.107654